Open access • Journal Article • DOI:10.1152/AJPRENAL.00228.2007

Phosphate transporters: a tale of two solute carrier families. — Source link

Leila V. Virkki, Jiirg Biber, Heini Murer, Ian C. Forster

Institutions: University of Zurich

Published on: 01 Sep 2007 - American Journal of Physiology-renal Physiology (American Physiological Society)

Topics: Cotransporter and Solute carrier family

Phosphate transporters: a tale of two solute carrier families

Virkki, L V; Biber, J; Murer, H; Forster, I C

Phosphate transporters: a tale of two solute carrier families

Abstract

Phosphate is an essential component of life and must be actively transported into cells against its electrochemical gradient. In vertebrates, two unrelated families of Na+ -dependent P(i) transporters carry out this task. Remarkably, the two families transport different P(i) species: whereas type II Na+/P(i) cotransporters (SCL34) prefer divalent HPO(4)(2-), type III Na(+)/P(i) cotransporters (SLC20) transport monovalent H2PO(4)(-). The SCL34 family comprises both electrogenic and electroneutral members that are expressed in various epithelia and other polarized cells. Through regulated activity in apical membranes of the gut and kidney, they maintain body P(i) homeostasis, and in salivary and mammary glands, liver, and testes they play a role in modulating the P(i) content of luminal fluids. The two SLC20 family members PiT-1 and PiT-2 are electrogenic and ubiquitously expressed and may serve a housekeeping role for cell P(i) homeostasis; however, also more specific roles are emerging for these transporters in, for example, bone mineralization. In this review, we focus on recent advances in the characterization of the transport kinetics, structure-function relationships, and physiological implications of having two distinct Na+/P(i) cotransporter families.

Am J Physiol Renal Physiol 293: F643–F654, 2007.
First published June 20, 2007; doi:10.1152/ajprenal.00228.2007.

Invited Review

Phosphate transporters: a tale of two solute carrier families

Leila V. Virkki, Jürg Biber, Heini Murer, and Ian C. Forster

Institute of Physiology and Center for Integrative Human Physiology (ZIHP), University of Zurich, Zurich, Switzerland

Submitted 16 May 2007; accepted in final form 14 June 2007

Virkki LV, Biber J, Murer H, Forster IC. Phosphate transporters: a tale of two solute carrier families. *Am J Physiol Renal Physiol* 293: F643–F654, 2007. First published June 20, 2007; doi:10.1152/ajprenal.00228.2007.—Phosphate is an essential component of life and must be actively transported into cells against its electrochemical gradient. In vertebrates, two unrelated families of Na^+-dependent P_i transporters carry out this task. Remarkably, the two families transport different P_i species: whereas type II Na^+/P_i cotransporters (SCL34) prefer divalent HPO_4^{2-}, type III Na^+/P_i cotransporters (SLC20) transport monovalent $H_2PO_4^-$. The SCL34 family comprises both electrogenic and electroneutral members that are expressed in various epithelia and other polarized cells. Through regulated activity in apical membranes of the gut and kidney, they maintain body P_i homeostasis, and in salivary and mammary glands, liver, and testes they play a role in modulating the P_i content of luminal fluids. The two SLC20 family members PiT-1 and PiT-2 are electrogenic and ubiquitously expressed and may serve a housekeeping role for cell P_i homeostasis; however, also more specific roles are emerging for these transporters in, for example, bone mineralization. In this review, we focus on recent advances in the characterization of the transport kinetics, structure-function relationships, and physiological implications of having two distinct Na^+/P_i cotransporter families.

phosphate; cotransport; electrophysiology; structure-function

PHOSPHORUS IS AN ESSENTIAL element of all living organisms and fulfills both structural and metabolic roles. Cells obtain phosphorus in the form of negatively charged inorganic phosphate (P_i) from the extracellular environment by means of secondary-active transport. In vertebrates, P_i transporters use the inwardly directed electrochemical gradient of Na^+ ions, established by the Na^+-K^+-ATPase, to drive P_i influx. Because defects in P_i homeostasis result in severe pathologies, it is essential to understand the transport mechanisms at the molecular level.

In this review, we focus on two unrelated families of mammalian phosphate transporters with an emphasis on the current state of knowledge about their structure and mechanistic properties at the molecular level and their physiological roles. Both are secondary-active, Na^+-coupled, yet their transport mechanisms are different. Proteins of the solute carrier family SLC34 (also called type II Na/P_i cotransporters) are the most extensively characterized in terms of function, structure, and regulation: its members play essential physiological roles in the kidney and small intestine for maintaining P_i homeostasis (for a review see Refs. 30 and 70). Proteins belonging to the SLC20 family (also called type III Na/P_i cotransporters) are represented by PiT-1 and PiT-2 and were originally identified as retroviral receptors (19). PiT-1 and PiT-2 are now emerging as important players in bone P_i metabolism and vascular calcification. Figure 1 compares the phylogeny of selected secondary-active P_i cotransport proteins belonging to the type II and type III families. The mammalian members are classified according to the human *SLC34* and *SCL20* gene family nomenclature.

A third transporter family, SLC17, is sometimes referred to as the type I Na^+-dependent P_i transporter family. The first cloned member of this family (NaPi-1) was first thought to be a Na^+-dependent P_i transporter based on *Xenopus laevis* oocyte expression studies (117) but was later shown to transport organic anions (14). Another SLC17 protein, BNP1, was also first classified as a Na^+/P_i transporter but was later shown to be a vesicular glutamate transporter (6). As no SLC17 family members are known to be strict Na^+/P_i cotransporters, they will not be reviewed further here (for a review of SLC17 see Ref. 82).

SLC34: Type II Na^+/P_i Cotransporter Family

Discovery and tissue distribution. Members of the SLC34 family, designated type II Na^+/P_i cotransporters (NaPi-II), are generally found in apical membranes of epithelia and epithelial-like cells. Early transport studies using membrane vesicles from renal and intestinal epithelial tissue documented secondary-active, Na^+-dependent P_i transport. Further studies used both cloned transporters and native tissue to characterize the kinetics and regulation of Na^+/P_i transport (for a review, see Ref. 70). SLC34 proteins belong to one of three phylogenetically distinct branches that are distantly related to the bacterial *Vibrio cholerae* Na^+-dependent P_i transporter (Fig. 1*A*). The first family member (NaPi-IIa/SLC34A1) was identified by expression cloning using *X. laevis* oocytes (61), and immunohistochemistry confirmed its localization at the apical membrane of renal proximal tubular cells. NaPi-IIa protein was also detected in rat brain (69), osteoclasts (53), and osteoblast-like cells (59), suggesting a wider expression profile for this "renal"

Address for reprint requests and other correspondence: I. C. Forster, Institute of Physiology, Univ. of Zurich, Winterthurerstrasse 190, CH-8057 Zurich, Switzerland (e-mail: Iforster@access.uzh.ch).

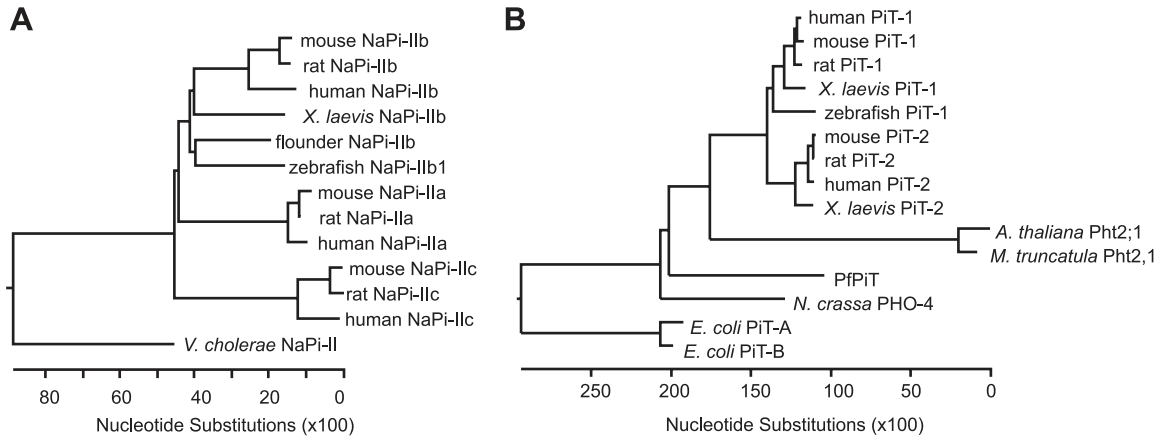

Fig. 1. Phylogenetic tree of SLC34 and SLC20 cotransporter families. Amino acid sequences were aligned using ClustalW. GenBank accession numbers are listed in parenthesis. *A*: SLC34 (type II Na^+/P_i transporters). The following sequences were used: mouse NaPi-IIb (AAC80007), rat NaPi-IIb (NP_445832), human NaPi-IIb (AAF31328), *Xenopus laevis* NaPi-IIb (AAF21135), human NaPi-IIa (AAA36354), flounder NaPi-IIb (AAB16821), mouse NaPi-IIc (NP_543130), rat NaPi-IIc (NP_647554), human NaPi-IIc (NP_543153), mouse NaPi-IIa (AAC52361), rat NaPi-IIa (NP_037162), human NaPi-IIa (AAA36354), and *Vibrio cholerae* NaPi-II (230325). *B*: SLC20 (type III Na^+/P_i transporters). The following sequences were used: human PiT-1 (NM_005415), mouse PiT-1 (AAB31458), rat PiT-1 (NM_031148), *X. laevis* PiT-1 (AAH59957), *Danio rerio* PiT-1 (NM_213179), mouse PiT-2 (NM_011394), rat PiT-2 (NM_017223), human PiT-2 (NM_006749), *X. laevis* PiT-2 (BC084098), *Arabidopsis thaliana* Pht2;1 (NM_113565), *Medicago truncatula* Pht2;1 (AAN46087), *Plasmodium falciparum* PfPiT (AJ580003), *Neurospora crassa* Pho-4 (XM_954396), *Escherichia coli* PitA (NC_002655), and *E. coli* PitB (NC_000913).

isoform. After the discovery of NaPi-IIa, a second isoform (NaPi-IIb/SLC34A2) was localized to the brush-border membrane of enterocytes and to lung, colon, testes, and liver (42). The third and newest member (NaPi-IIc/SLC34A3), like NaPi-IIa, is apically expressed in the renal proximal tubule (60, 89). The amino acid sequences of all three SLC34 proteins are similar in the predicted transmembrane-spanning regions but diverge in the NH_2 and COOH termini and a prominent extracellular loop that separates the protein into two halves (see *Topology and structure-function studies*).

Physiological role and pathophysiology. The expression and regulation of SLC34 proteins in their intestinal and renal context have been extensively studied because these organs represent, respectively, the principle entry and exit points for P_i. Renal regulation of NaPi-IIa has been the subject of several recent reviews (30, 66, 70, 98, 100, 116) and is briefly discussed here. The critical role of NaPi-IIa for P_i homeostasis is underscored by the hyperphosphaturia phenotype documented in the NaPi-IIa knockout mouse (5). Dysregulation of NaPi-IIa causes P_i deficiency disorders, such as X-linked hypophosphatemia (XLH) and autosomal-dominant hypophosphatemic rickets (ADHR) (reviewed in Ref. 98). However, no mutation in the NaPi-IIa gene *NPT2a* has yet been unequivocally linked to human disease. Prié et al. (78) reported that heterozygous mutations in NaPi-IIa were responsible for hypophosphatemia leading to nephrolithiasis or osteoporosis. They reported that the mutations caused a decrease in apparent P_i affinity or impaired targeting to the plasma membrane and induced a dominant negative effect on wild-type transporter function when expressed in *X. laevis* oocytes. In contrast, extensive investigation of the same mutants in our laboratory found no evidence for such effects (111). The present consensus is that the mutations alone are not responsible for the clinical disorders in the patients (98). Recently, a second study of NaPi-IIa genetic polymorphisms as a possible cause of hyperphosphaturia and hypercalciuria (55) reported no significantly altered kinetics of the mutant NaPi-IIa transporters when expressed in *X. laevis* oocytes.

In mice with homozygous deletion of the *Npt2a* gene, ~30% P_i reabsorption remains in the kidney. This fraction can most likely be attributed to NaPi-IIc, which was originally described as a growth-related transporter in weaning rats (89). Recent publications describe mutations of the *NPT2c* gene in humans as being responsible for hereditary hypophosphatemic rickets with hypercalciuria (HHRH) (7, 47, 57). The effect of mutations on the NaPi-IIc protein identified in patients diagnosed with HHRH is currently undergoing in vitro investigation (C. Bergwitz, personal communication). Interestingly, two of the mutants have amino acid substitutions that correspond to functionally important sites identified in the context of electrogenicity (Ref. 3 and see below). Moreover, the marked pathophysiological consequences of NaPi-IIc mutations in human subjects suggest a more important role for this protein than initially suspected from animal data (89).

Whereas the physiological roles of SLC34 proteins, particularly in the kidney, are well characterized, it is obvious that future work must also focus on other organs. For example, regulated P_i transport is crucial for the formation of mineralized bone. NaPi-IIa is expressed in osteoclasts (37, 53) and chondrocytes (62), whereas osteoblasts express both NaPi-IIa and NaPi-IIb (59). NaPi-IIb is responsible for transcellular P_i absorption in the small intestine and is regulated by dietary P_i (80) and metabolic acidosis (91). In the liver, NaPi-IIb is involved in the reabsorption of P_i from primary hepatic bile (35). In salivary glands, NaPi-IIb is involved in secreting P_i into saliva, where a high P_i content is important for remineralization of dental enamel (45). In the brain, NaPi-IIa may play a role in central nervous system regulation of P_i homeostasis (44, 69). Improper NaPi-IIb expression in the epididymis is implicated as a possible causative agent in a mouse model of male infertility (120). NaPi-IIb is expressed in alveolar type II cells (101), and mutations in NaPi-IIb have recently been associated with pulmonary microlithiasis (20, 46). In mice, NaPi-IIb is expressed apically in lactating mammary gland but not in virgin mice (67), which suggests a role for NaPi-IIb in milk secretion. Dysfunction of NaPi-IIb may also be involved

in the formation of microliths in other organs where the transporter is expressed. Of particular significance is that mammary tissue, microcalcifications containing calcium phosphate, are more commonly associated with malignancy than ones without a phosphate component (34).

Finally, although specific studies are still lacking, it is likely that the newcomer, NaPi-IIc, is not exclusively expressed in the kidney, as originally suggested (71, 89). A query of published microarray data deposited in the Gene Expression Omnibus (GEO) database reveals that the transcript for NaPi-IIc is abundant in several tissues, such as brain, breast, liver, and blood (L. V. Virkki, unpublished observations). Like for NaPi-IIa and NaPi-IIb, it is expected that future studies will reveal important roles for NaPi-IIc also in these extrarenal locations.

Transport kinetics. The transport kinetics of SLC34 proteins have been extensively studied (for a review, see Refs. 30 and 31) by means of heterologous expression in *X. laevis* oocytes. In essence, all three SLC34 proteins exhibit a strict dependence on external Na^+ as the driving substrate, with an apparent affinity for Na^+ of ~50 mM, a preference for divalent P_i (HPO_4^{2-}) as the driven substrate with an apparent affinity of ≤0.1 mM, and cotransport activity inhibitable by phosphonoformic acid (PFA) (15, 119; G. Stange, I. C. Forster, unpublished observations). These common features indicate that the basic transport mechanism is the same for all SLC34 members. Nevertheless, two important, interrelated differences in the kinetic properties have been documented, namely, electrogenicity and stoichiometry. NaPi-IIa and NaPi-IIb are electrogenic, and transport P_i with a 3:1 Na^+:HPO_4^{2-} stoichiometry, whereas NaPi-IIc is electroneutral and operates with a 2:1 Na^+:HPO_4^{2-} stoichiometry.

ELECTROGENIC ISOFORMS NaPi-IIa/b. Tracer uptake assays on brush-border membrane vesicles first suggested that Na^+-coupled P_i cotransport was electrogenic (12). However, this property could not be unequivocally defined without determination of the Na^+-P_i stoichiometry, identification of the preferred P_i species, and transmembrane electrical measurements. More direct evidence for electrogenic Na^+-dependent P_i cotransport was obtained by recording the transmembrane potential of isolated, perfused proximal tubule cells (88), later confirmed by heterologous expression of cloned NaPi-IIa in *X. laevis* oocytes (13, 39). These studies established that P_i induced an inward current in the presence of external Na^+ when the cell was hyperpolarized (Fig. 2, *A* and *B*). By assuming that the P_i-induced change in cell holding current under voltage clamp (I_{Pi}) directly reflected the cotransport activity, it was inferred that NaPi-IIa operated with a 3:1 Na^+:P_i stoichiometry at physiological pH (7.4), where divalent P_i predominates. Nevertheless, there was uncertainty about the selectivity of the transporter for divalent vs. monovalent P_i and the influence of external pH, which itself determines the availability of the P_i species. Simultaneous measurement of net charge transfer and substrate flux (32, 110) and surface pH measurements (81) (see Fig. 6*C*) on the same oocyte have resolved this issue unam-

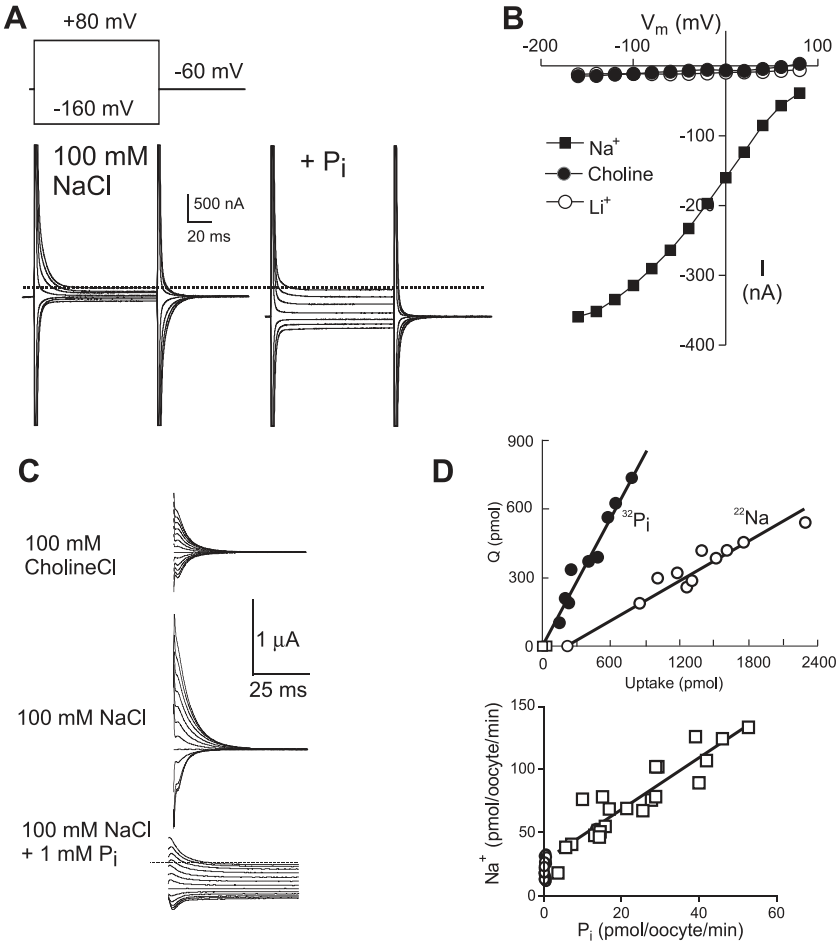

Fig. 2. Basic transport properties of SLC34 proteins expressed in *X. laevis* oocytes. *A*: original current recordings from an oocyte expressing flounder NaPi-IIb in solution containing 100 mM Na^+ (*left*) and 100 mM Na^+ 1 mM P_i (*right*). The voltage was stepped from −160 to +80 mV in 40-mV increments. *B*: characteristic current-voltage curve for P_i-dependent currents (I_{Pi}) with different driving cations (at 100 mM) for an oocyte expressing the flounder NaPi-IIb isoform. Each data point is the difference between the oocyte holding current at the indicated membrane potential with and without 1 mM P_i (pH 7.4). No significant inward current is recorded when Na^+ is replaced with choline or Li^+. *C*: pre-steady-state relaxations recorded from an oocyte expressing the flounder NaPi-IIb isoform evoked by voltage steps from −60 mV to voltages in range −180 to +80 mV. Relaxations are partially suppressed in presence of 1 mM P_i, and in 100 mM cholineCl, relaxations are still resolvable. These are thought to arise from molecular rearrangements within the NaPi-IIb protein. *D*: determination of the stoichiometry of SLC34 proteins. *Top*: individual oocytes expressing the electrogenic rat NaPi-IIa isoform were voltage clamped, and the charge (Q) and amount of tracer substrate ($^{32}P_i$ or ^{22}Na) taken up was assayed. The ratio Q:P_i (filled symbols) is ~1:1, the ratio Q:Na (open symbols) is ~1:3. These data indicate that the Na:P_i stoichiometry is 3:1, with one net charge translocated per P_i. (redrawn and modified from Ref. 32). The Q:P_i ratio remains unchanged at lower pH, indicating that divalent P_i is the preferred species (not shown). *Bottom*: for electroneutral NaPi-IIc, data indicate a ratio Na:P_i of 2:1, consistent with a preference for divalent P_i and 2 Na^+ ions translocated per cycle (redrawn and modified from Ref. 3).

biguously. Moreover, these studies confirmed that NaPi-IIa and NaPi-IIb preferentially transport divalent P_i, independently of the external pH (Fig. 2*D*) (32). External acidification affects both the intrinsic voltage dependence and Na^+ interaction of electrogenic NaPi-II cotransporters (29, 110), which results in a decrease in maximum transport rate and reduced apparent affinity for divalent P_i (see Fig. 6*A*).

The electrogenicity of NaPi-IIa/b implies that net charge is transported across the membrane. Moreover, I_{Pi} shows rate-limiting, voltage-independent behavior at hyperpolarizing and depolarizing extremes (Fig. 2*B*). This indicates that the transport cycle involves both voltage-dependent and voltage-independent partial reactions. The former have been identified from analysis of pre-steady-state charge movements evoked by voltage steps (for a review, see Ref. 31) (Fig. 2*C*). For carrier proteins like NaPi-IIa/b, the charge movements in the absence of substrate are proposed to reflect two events: *1*) a major reorientation of the carrier that alternately exposes the substrate binding sites to the external or internal medium and *2*) movement of Na^+ ions from the external milieu to and from their binding site(s) within the transmembrane field (30, 31).

The transport turnover rate of NaPi-IIa/b can be estimated from pre-steady-state and steady-state data. Rates in the range 4–10 s^{-1} at 20°C are predicted (33) and should be about threefold faster under normal physiological conditions, when the temperature dependence of the kinetics is taken into account (2). Combining steady-state and pre-steady-state data has led to the proposal of an ordered kinetic scheme for the NaPi-IIa/b transport cycle (28, 33, 110, 113) (see Fig. 7*A*). Voltage dependence is conferred by the empty carrier and one Na^+ binding transition. Similar schemes have been proposed for other Na^+-coupled solute carriers [e.g., Na^+/glucose transporter SGLT1 (76) and Na^+/iodide transporter NIS (23)] and are consistent with the alternating access mechanism for transmembrane transport. Previously, a single Na^+ ion was assumed to interact with the protein before P_i binding (28). The model was revised to incorporate new evidence obtained by simultaneous whole-oocyte electrophysiology and time-resolved fluorescence of a site-directed fluorescent label (voltage clamp fluorometry; VCF) (113) that identified an additional, electrically silent, Na^+ binding transition preceding P_i binding.

ELECTRONEUTRAL NaPi-IIC. The electroneutrality of NaPi-IIc (71, 89) comes as a surprising contrast to the voltage dependence of NaPi-IIa/b, and this fact emphasizes how small differences in amino acid composition can drastically alter specific kinetic properties. Oocytes expressing functional NaPi-IIc (confirmed by $^{32}P_i$ uptake) are electrically silent (3, 89). For other kinetic properties, such as apparent substrate

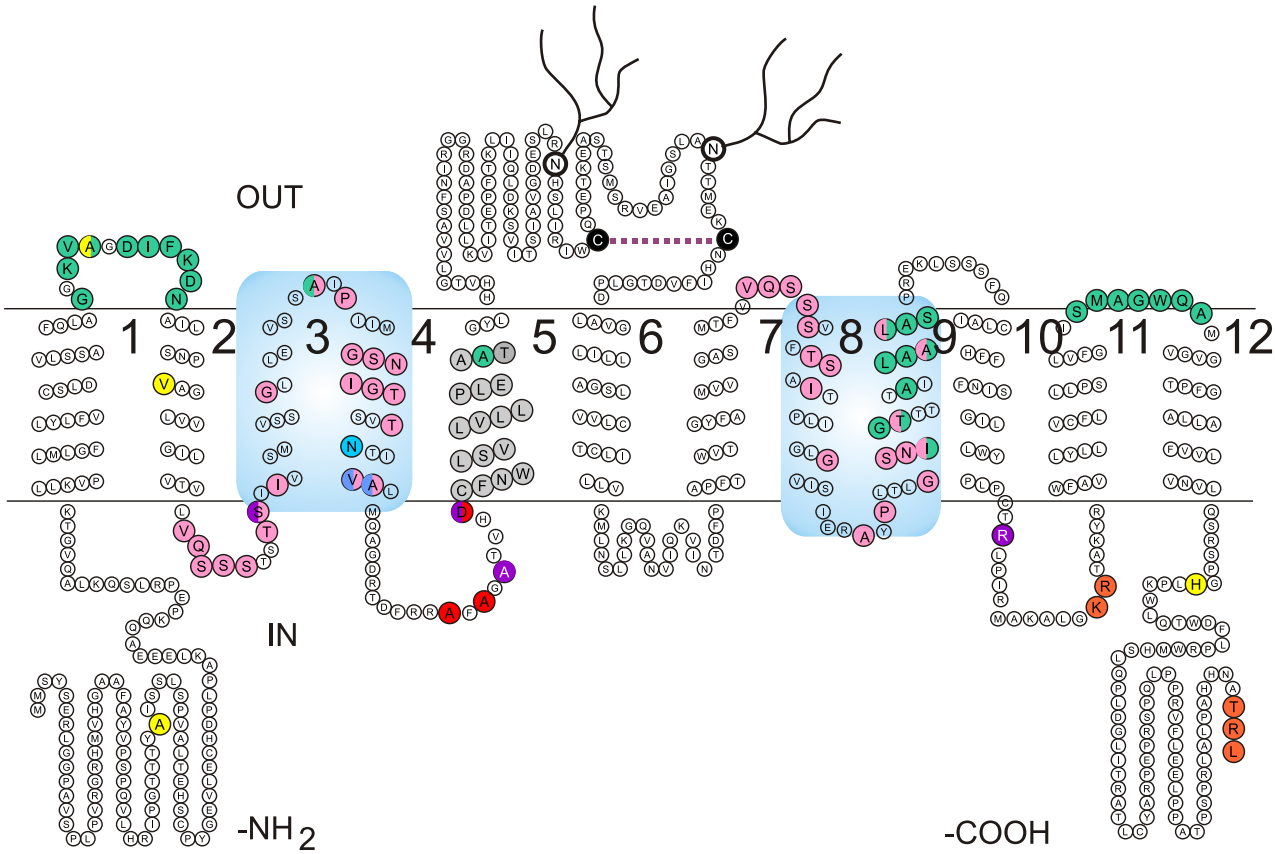

Fig. 3. Topological model for rat NaPi-IIa. Transmembrane domains were assigned according to Ref. 79. The model was drawn with the aid of TOPO2 software (http://www.sacs.ucsf.edu/TOPO/topo.html). Enlarged symbols indicate sites of significant structure-function importance. Pink, identical residues in the NH_2- and COOH-terminal repeated regions (see text); green, sites that are, when mutated to a cysteine, accessible to the extracellular milieu; blue, sites that are, when mutated to a cysteine, accessible to the intracellular milieu; red, sites important for electrogenicity; orange, sites important for regulation and targeting; yellow, sites of naturally occurring SLC34A1 (human NaPi-IIa) mutants shown not to affect function; purple, equivalent sites of reported naturally occurring SLC34A3 (human NaPi-IIc) mutations. An essential disulfide bridge in the large extracellular loop is indicated (dashed line). Light blue regions are reentrant loops, proposed to form a putative transport pathway through the protein. Two *N*-glycosylation sites have been identified in the large extracellular loop.

affinity and pH dependence, NaPi-IIc is indistinguishable from its electrogenic cousins. Moreover, its Na^+:P_i stoichiometry of 2:1 is consistent with a preference for divalent P_i and is thus similar to NaPi-IIa and IIb (Fig. 2*D*) (3). Thus NaPi-IIc lacks one of the three Na^+ interaction steps proposed for NaPi-IIa/b. Simulations of the transport steady-state and pre-steady-state kinetics also support the notion that the first Na^+ interaction may be electrogenic, followed by an electroneutral or weakly electrogenic second Na^+ interaction (see Fig. 7*A*). The latter would correspond to the first Na^+ interaction for NaPi-IIc (I. C. Forster, unpublished observations).

Topology and structure-function studies. The current topological model of SLC34 has been developed mainly using cysteine scanning and in vitro transcription/translation on NaPi-IIa but is probably applicable also to NaPi-IIb and NaPi-IIc (for a review, see Refs. 30 and 31). The model comprises 12 transmembrane-spanning domains, intracellularly located NH_2 and COOH termini, and two *N*-glycosylation sites located in a large extracellular loop (Fig. 3). NaPi-IIa is a functional monomer (54), and this is also assumed to be the case for NaPi-IIb and NaPi-IIc. There is evidence for in vivo dimerization of SLC34 proteins from dual tagging and split ubiquitin approaches and freeze fracture studies on *X. laevis* oocytes expressing the flounder NaPi-IIb isoform (30). At present, the tertiary structure of the monomers is unknown; however, at least one disulfide bridge is essential for stable expression of NaPi-IIa in the oocyte membrane (Fig. 3). This may play a role in defining the spatial arrangement of the transmembrane domains. Sites specific to expression and residues critical for regulation have been identified on the intracellular side (Fig. 3): the KR motif confers PTH sensitivity, and a TRL/THL motif, which is a PDZ binding motif, found in the COOH-terminal tail is essential for membrane expression (for a detailed review, see Refs. 30 and 41).

An important structural feature of the NaPi-II primary sequence are the two "repeat" regions in the NH_2- and COOH-terminal halves of the protein. These repeats are preserved in all NaPi-IIa/b/c transporters as well as in homologs from *V. cholerae* and *Caenorhabditis elegans* (116), which strongly suggests that this conserved motif plays an essential functional role. The current secondary topology of NaPi-IIa depicts these regions as incorporating two pairs of α-helices. Further studies have demonstrated that they may form two opposed reentrant loops that create opposed vestibules, allowing substrate access from either side of the membrane (79, 112).

Recent VCF data also support the notion that the two halves of the NaPi-IIb protein move in a complementary manner during the transport cycle (112). The dependence of fluorescence on substrate and membrane potential, recorded from four labeled sites located in externally accessible linker regions, indicated that complementary conformational changes occur in the two halves of the protein during the transport cycle. VCF studies offer a real-time, albeit indirect, view of molecular rearrangements that occur at specific sites during substrate interaction and translocation.

Finally, the difference in electrogenicity between NaPi-IIa/b and NaPi-IIc was exploited to identify a charged residue that is most likely implicated in Na^+ binding and electrogenicity of NaPi-IIa/b (3) (Fig. 3). A sequence alignment revealed three clusters of residues that differed between the NaPi-IIa/b and NaPi-IIc isoforms. One cluster contained an aspartic acid (Asp-224 in human NaPi-IIa) conserved in all electrogenic isoforms but replaced by a glycine (Gly-196 in human NaPi-IIc). When three amino acids in NaPi-IIc (including Gly-196) were replaced with the corresponding amino acids of NaPi-IIa/b, electrogenic P_i transport was conferred to NaPi-IIc. Consistent with expectations, pre-steady-state charge movements were also detected. Signifi-

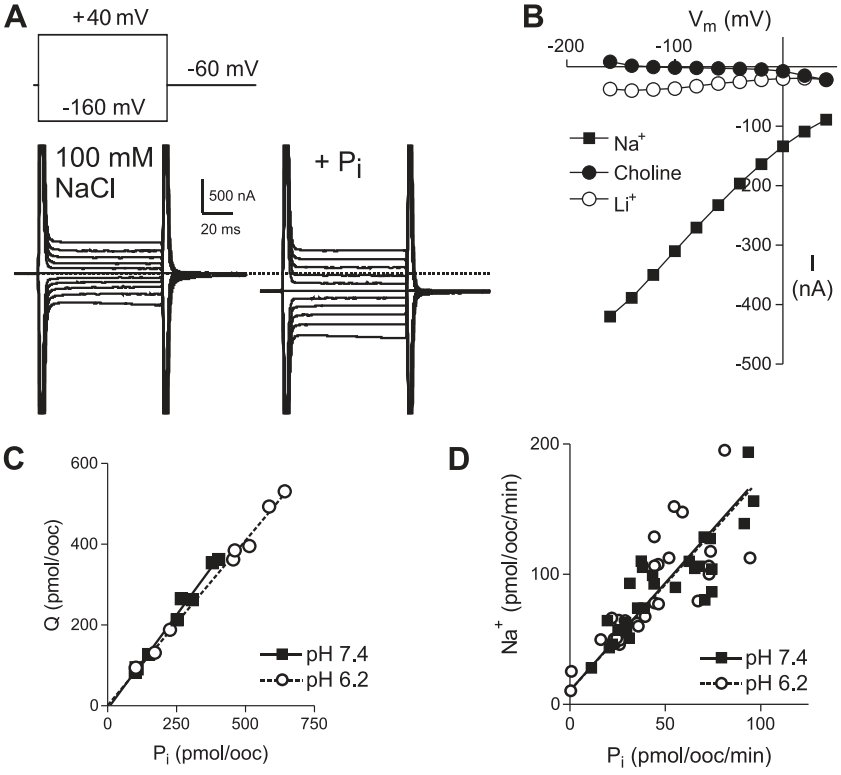

Fig. 4. Basic transport properties of SLC20 proteins expressed in *X. laevis* oocytes. *A*: original current recordings from an oocyte expressing *X. laevis* PiT-1 in solution containing 100 mM Na^+ (*left*) and 100 mM Na^+ and 1 mM P_i (*right*). The voltage was stepped from −160 to +40 mV in 20-mV increments. *B*: characteristic current-voltage curve I_{Pi} derived from data in *A* with different driving cations (at 100 mM) for an oocyte expressing the *X. laevis* PiT-1 isoform. No significant inward current is recorded when Na^+ is replaced with choline, whereas in Li^+ currents are reduced by ~85% at negative membrane potentials, compared with Na^+. *C*: data for the determination of the *Q*:P_i stoichiometry of *X. laevis* PiT-1. Individual oocytes expressing XlPiT-1 were voltage clamped, and the charge (*Q*) and amount of P_i translocated were assayed by integrating the P_i-induced current and by using $^{32}P_i$ as a tracer, respectively. The ratio *Q*:P_i was ~1:1 at both pHs assayed (7.4 and 6.2). *D*: data for the determination of the Na^+:P_i stoichiometry of *X. laevis* PiT-1. Dual uptake assay with ^{22}Na and $^{32}P_i$ as tracers performed at pH 6.2 and 7.4 suggests a 2:1 Na^+:P_i stoichiometry for SLC20. Since the *Q*:P_i and Na^+:P_i ratios were the same at both pH, monovalent P_i should be the preferred species. *C* and *D* were redrawn and modified from Ref. 81.

cantly, the Na^+:P_i stoichiometry of the electrogenic mutant NaPi-IIc is 3:1; however, its apparent substrate affinities and voltage dependence are altered compared with wild-type transporters. Furthermore, replacing the conserved Asp-224 in NaPi-IIa with NaPi-IIc's glycine resulted in electroneutral P_i transport, thus confirming that Asp-224 is necessary for a 3:1 Na^+:P_i stoichiometry (109).

SLC20: Type III Na^+/P_i Cotransporter Family

Discovery. Type III Na^+/P_i cotransporters were first identified as receptors for retroviruses, which may enter a cell following a specific interaction with the receptor. The first hint that the retroviral receptor Glvr-1, which renders cells susceptible to infection by gibbon ape leukemia virus, is a phosphate transporter was revealed by its homology to a phosphate permease from *Neurospora crassa*, a filamentous fungi (48). A related protein, which renders cells susceptible to infection by amphotropic murine retrovirus (Ram-1) was subsequently identified (65, 104). Experimental evidence showing that retroviral receptors Glvr-1 and Ram-1 are electrogenic Na^+/P_i symporters then followed (51, 52, 72), and the receptors were renamed PiT-1 and PiT-2, respectively.

PiT-1- and PiT-2-related proteins are present in all phyla (Fig. 1*B*). In prokaryotes and in plants, P_i transport is coupled to the H^+ gradient (21, 38, 103), whereas in animals and fungi, the driving cation is Na^+ (19, 64, 106). In the bacterium *Bacillus subtilis*, the related protein CysP mediates H^+/SO_4^{2-} cotransport (63), but so far no other PiT family member has been shown to transport SO_4^{2-}.

Physiological role and pathophysiology. PiT proteins have a broad tissue distribution, and it was proposed that they serve a housekeeping function in cells. At the mRNA level, PiT-1 and PiT-2 are ubiquitously but differentially expressed in different tissues (4, 97, 102). However, recently more specific roles for PiT proteins in various physiological and pathophysiological processes have emerged. For example, PiT-mediated P_i transport appears to play an important role in providing P_i for the formation of mineralized bone (16, 36, 75, 93, 121, 123). Accordingly, it has been shown that in cultured bone-derived cells P_i transport and PiT mRNA levels are regulated by various factors, such as P_i, epinephrine, platelet-derived growth factor (PDGF), insulin-like growth factor (IGF-1), and basic fibroblast growth factor (bFGF) in osteoblast-like cells (18, 94, 95, 122, 123) and in chondrogenic cells by transforming growth factor-β (TGF-β) (74) as well as P_i levels (114). Interestingly, P_i regulation of PiT-2 transport function may result from posttranslational modification of the transporter (83), and P_i may regulate the formation of PiT-2 oligomers, implying that PiT proteins play a role in phosphate sensing (84). In addition to playing a role in normal calcification, PiT

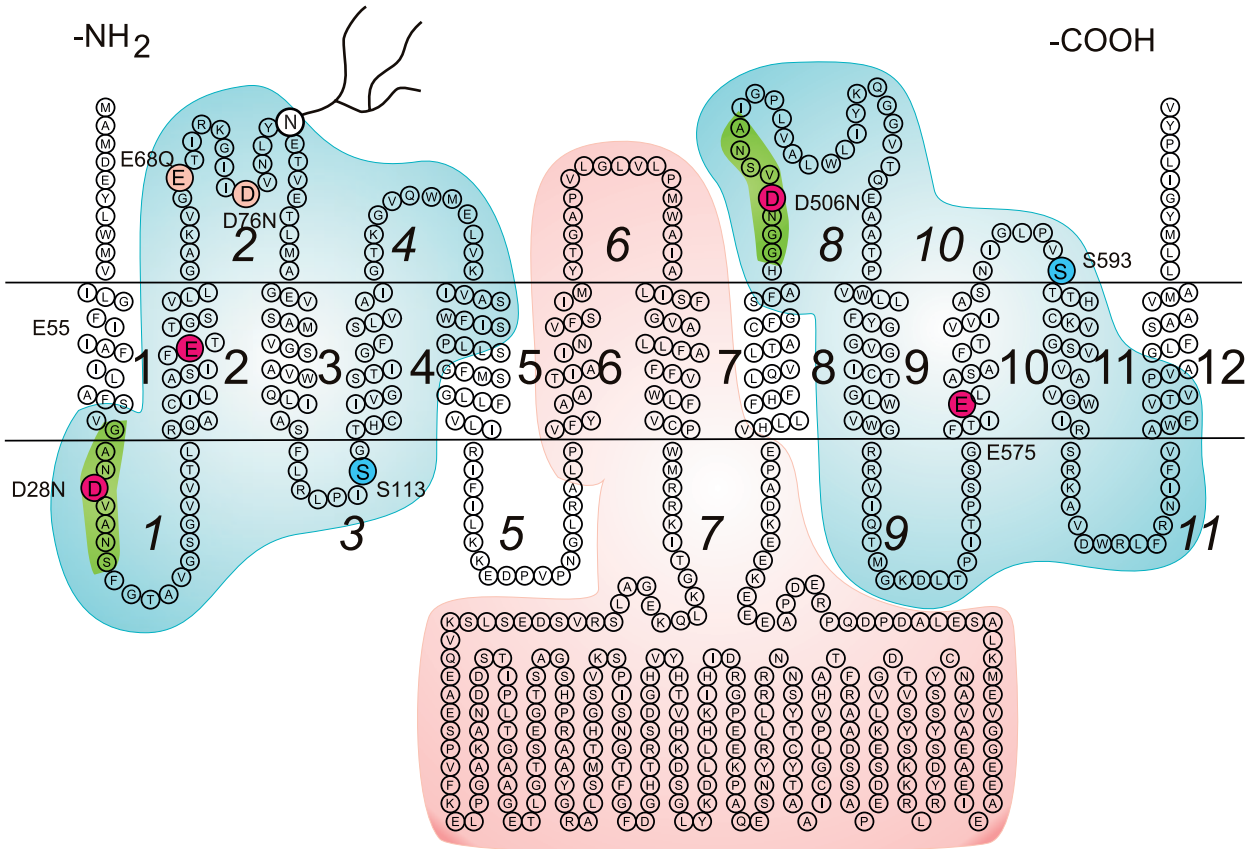

Fig. 5. Topological model for human PiT-2. Transmembrane domains were assigned according to Ref. 86. The model was drawn with the aid of TOPO2 software (http://www.sacs.ucsf.edu/TOPO/topo.html). Residues important to PiT function investigated by mutagenesis (10, 11, 85) are indicated. Light blue, PD1131 homology domains identified in Ref. 86; pink, region that can be removed without compromising retroviral receptor function of PiT-2 (9). Red, acidic residues important for transport function (D28, E55, D506, E575) and not critical for transport function (E68, D78, E91). The protein is *N*-glycosylated at Asp-81. Numbers designate predicted transmembrane domains and loops (italic) referred to in the text.

Table 1. *Properties of Na^+/P_i cotransporters*

	Substrates	Stoichiometry Na^+:Pi	Electrogenic	Concentrating Capacity	PFA Block	Mutations Associated with Disease
NaPi-IIa	Na^+, HPO_4^{2-}, Arsenate	3:1	Yes	10,000	Yes	
NaPi-IIb	Na^+, HPO_4^{2-}, Arsenate	3:1	Yes	10,000	Yes	Pulmonary Alveolar Microlithiasis (20, 46)
NaPi-IIc	Na^+, HPO_4^{2-}, Arsenate	2:1	No	100	Yes	HHRH (7, 47, 57)
PiT-1	Na^+, $H_2PO_4^-$, Li^+, Arsenate	2:1	Yes	1,000	No	
PiT-2	Na^+, $H_2PO_4^-$, Li^+, Arsenate	2:1	Yes	1,000	No	

Concentration capacity is shown for a membrane potential of −60 mV and a 10-fold Na^+ gradient (outside-inside). HHRH, hereditary hypophosphatemic rickets with hypercalciuria. References are shown in parentheses.

proteins were recently implicated in pathological processes, such as hyperphosphatemia-induced calcification of vascular tissue (50, 56, 68) and osteoarthritis (17).

Regulation of PiT function has also been shown for extraskeletal cells and tissues. For example, in human embryonic kidney cells (HEK-293), PiT-1-mediated P_i transport is regulated by P_i levels and PTH (25). In rat parathyroid glands, PiT-1 mRNA levels are regulated by plasma vitamin D and P_i levels (97).

Unfortunately, at the protein level only limited data are available regarding the tissue and subcellular distribution of PiT-1 and PiT-2. Khadeer et al. (53) detected PiT-1 mRNA in osteoclasts and macrophages and showed that transfected protein localizes to the basolateral membrane. This subcellular localization was similar to that of NaPi-IIa, indicating an involvement of both NaPi-IIa and PiT-1 in P_i transport in bone-resorbing osteoclasts. PiT proteins may also play a role in P_i transport in the distal segments of the kidney. Tenenhouse et al. (99) showed that both PiT-1 and PiT-2 mRNAs are present in immortalized mouse distal convoluted tubule (MDCT) cells and that the pH dependence of P_i transport is consistent with PiT-mediated transport.

Finally, PiT proteins may play an important role in basolateral as well as apical P_i uptake in polarized epithelia. In the liver, PiT-1 and PiT-2 localize to the basolateral membrane in hepatocytes (35), whereas in airway epithelial cells PiT-2 is expressed both apically and basolaterally (115). In P_i-secreting glands, such as the lactating mammary gland (90) and ruminant parotid gland (105), PiT proteins may provide basolateral uptake of P_i from the blood for subsequent secretion into the lumen through an as yet unknown mechanism.

Recently, Saliba et al. (87) showed that the malaria parasite *Plasmodium falciparum* expresses a PiT protein (PfPiT) in its plasma membrane that is instrumental for supplying P_i to the intraerythrocytic parasite. PfPiT-mediated P_i transport is energized by the Na^+ gradient and, because infection causes a gradual increase in intracellular Na^+, there is adequate driving force for P_i uptake via PfPiT.

Transport kinetics. After Kavanaugh et al. (52) in 1994 showed that the retroviral receptors Glvr-1 and Ram-1 are electrogenic Na^+/P_i cotransporters, very limited characterization of the transport kinetics of either PiT-1 or PiT-2 has been reported (4, 8, 97, 99, 107). None of these more recent studies used electrophysiology, which is essential for the kinetic characterization of electrogenic transporters. Furthermore, these studies suffered from low transport activities, possibly because of low expression. To close this knowledge gap, we recently characterized PiT transport kinetics using the *X. laevis* oocyte expression system and two-electrode voltage clamp as well as radiotracer uptake (81). We performed most of our kinetic studies on a *X. laevis* PiT-1 clone (XlPiT-1), which gave much

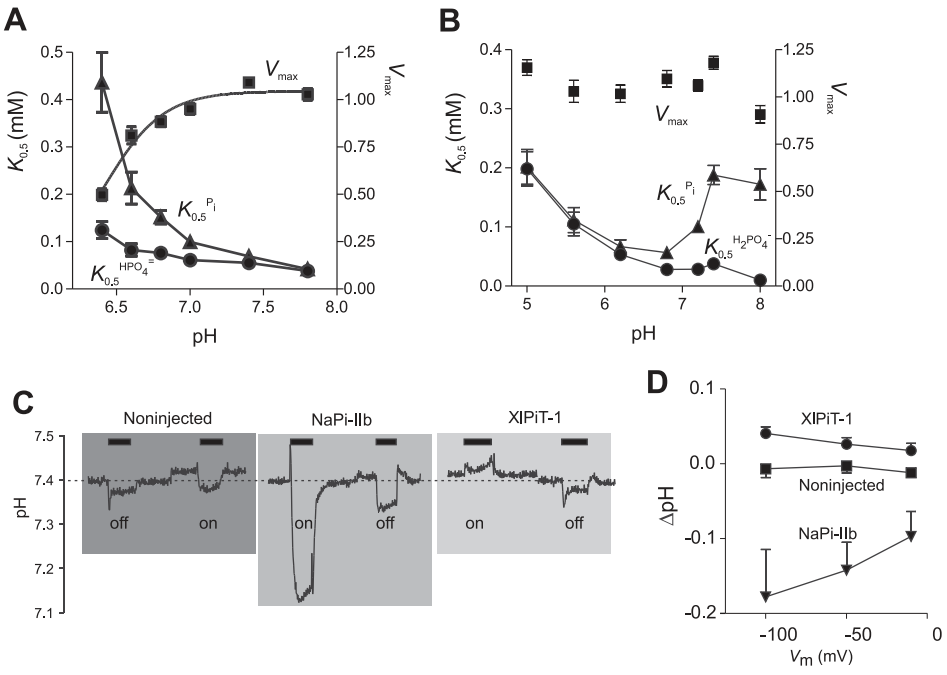

Fig. 6. pH and transport characteristics of SLC34 and SLC20 compared. *A*: P_i and HPO_4^{2-} apparent affinities ($K_{0.5}$) and maximum transport rate (V_{max}) measured in oocytes expressing human NaPi-IIa as a function of pH. V_{max} data were fitted with the Hill equation, yielding an apparent inhibitory constant K_i for H^+ of 400 ± 40 nM with a Hill coefficient of −2.1 ± 0.6 (110). *B*: P_i and $H_2PO_4^-$ $K_{0.5}$ and V_{max} measured in oocytes expressing XlPiT as a function of pH. *C*: surface pH measurements in noninjected oocytes and in oocytes expressing flounder NaPi-IIb or XlPiT. Application of 1 mM P_i is indicated by a filled bar. ON and OFF refers to the pH electrode position: either pressed against the oocyte or in the bath, respectively. *D*: summary of surface pH changes induced by P_i application in experiments similar to *C*. pH changes in oocytes expressing either NaPi-IIb or XlPiT are significantly different from uninjected oocytes. Data in *B–D* are redrawn from Ref. 81.

higher P_i transport in *X. laevis* oocytes than mammalian PiT-1 or PiT-2.

In XlPiT-1-expressing oocytes, applying P_i in the presence of Na^+ induces an inward current (I_{Pi}) with no reversal potential over the voltage range applicable to oocytes (−180 to + 80 mV; Fig. 4*B*). PiT-dependent P_i transport is Na^+ dependent, but Li^+ supports P_i transport to a small extent (11, 81, 107). Interestingly, two studies have shown that in the absence of Na^+, lowering pH from 7.5 to 6.0 induced significant P_i uptake in oocytes expressing PiT-2, indicating that in this isoform H^+ could substitute for Na^+ (8, 107). Li^+ may support cotransport in some Na^+-driven transporters, such as the Na^+/dicarboxylate transporter (73), Na^+-driven Cl^-/HCO_3^- exchanger (108), and the Na^+/glucose cotransporter (43), but not in type II Na^+/P_i cotransporters, although Li^+ may interact with their transport cycle (112, 113).

Another difference between type II and type III Na^+/P_i cotransporters is that whereas Na^+-dependent pre-steady-state currents are readily measured in oocytes expressing NaPi-IIa or NaPi-IIb in the absence of P_i, analogous charge movement in oocytes expressing XlPiT-1 were undetectable, although I_{Pi} was of similar magnitude as in NaPi-II-expressing cells (Fig. 4, *A* and *B*). PiT-1 pre-steady-state relaxations may be too fast to detect and remain buried in the capacitive transient of the oocyte or indicate that other models of electrogenic transport should be considered.

Neither PiT-1 nor PiT-2 transports sulfate; however, the toxic phosphate mimetic arsenate interacts with PiT-1 (4, 52, 81). Arsenate competes with P_i and reduces P_i transport in both PiT-1 and PiT-2 and also induces inward currents similar to P_i but has a lower affinity (4, 81). The effects of arsenate are very similar in type II Na^+/P_i cotransporters (15, 39).

The transport stoichiometry of XlPiT-1 was determined by combining electrophysiology and ^{22}Na and $^{32}P_i$ tracer uptake experiments. PiT-1 transports two Na^+ ions for each monovalent $H_2PO_4^-$ with one positive charge (81) (Fig. 4, *C* and *D*). We confirmed that $H_2PO_4^-$ is preferred over HPO_4^{2-} in PiT-1, using surface pH measurements. Because removal of either $H_2PO_4^-$ or HPO_4^{2-} from the medium by a transporter causes a shift in $H_2PO_4^-$:HPO_4^{2-} equilibrium, a measurable change in H^+ concentration occurs. For oocytes expressing PiT-1, application of 1 mM P_i caused alkalinization at the oocyte surface, consistent with transport of $H_2PO_4^-$ into the cell (see Fig. 6*C*). In contrast, expressing the type II Na^+/P_i cotransporter resulted in acidification, in agreement with transport of HPO_4^{2-} (see Fig. 6, *C* and *D*).

PiT proteins are less sensitive to H^+ than members of the SLC34 family. The maximum attainable P_i transport rate (V_{max}) is not influenced by changes in pH between 5.0 and 7.4 (see Fig. 6*B*). Whereas the apparent affinity for total P_i shows a biphasic change with pH with a minimum ~pH 6.8, the apparent affinity for the preferred substrate HPO_4^{2-} is reasonably constant between pH 6.2 and 8.0 and decreases at more acidic pH. In contrast, P_i transport mediated by members of the type II cotransporter family (see Fig. 6*A*) is strongly reduced at acidic pH due to the inhibitory effect of protons on the transport cycle as well as reduced availability of divalent HPO_4^{2-} (29, 110). Thus PiT proteins can maintain high P_i transport capacity even at the highly acidic pH of 5.0, where SLC34 transporters no longer function.

Presently, there are no known inhibitors of PiT-mediated P_i transport. Phosphonoformic acid (PFA) is a well-known inhibitor of Na^+-dependent P_i transport mediated by type II Na^+/P_i cotransporters (15, 96), but it does not inhibit PiT-1 or PiT-2 when expressed in oocytes (81). Although inhibition by PFA of PiT-mediated P_i transport has been reported (4, 99, 107), only high concentrations (≥10 mM) were effective and membrane potential was not controlled, so the effect of PFA may have been nonspecific. In addition, it has been reported that PFA blocks P_i-induced calcification in smooth muscle cells (50, 56) as well as matrix calcification in osteoblast-like cells (93) and osteoblast subcultures (121). As PFA does not block PiT-mediated P_i transport, it is likely that this effect is due to the ability of phosphonates and bisphosphonates to inhibit calcium crystal formation (26, 27, 118). Alternatively, a member of the PFA-sensitive type II Na/Pi cotransporter family may play a role in the calcification process.

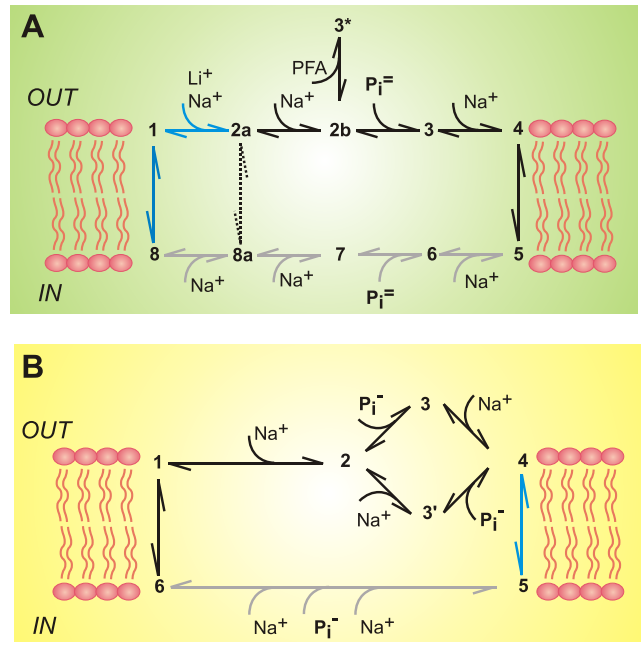

Fig. 7. Kinetic schemes for SLC34 (*A*) and SLC20 (*B*) proteins based on the interpretation of experimental data. Numbers indicate conformational states of the protein. Light grey indicates transitions for intracellularly facing conformational changes that are uncharacterized. *A*: electrogenic SLC34 proteins (NaPi-IIa/b) obtain their electrogenicity from the empty carrier reorientation (*8-1*) and binding of 1 Na^+ ion within the transmembrane electric field (*1-2a*). Li^+ can also interact with the protein when in *state 1* and possibly prevents subsequent transitions from occurring. An electroneutral second Na^+ binding step precedes the P_i interaction (*2a-2b*). The fully loaded carrier is electroneutral (intrinsic carrier charge $+3Na^+ + H_2PO_4^-$) and the reorientation (*4-5*) is proposed to be rate limiting. Phosphonoformic acid (PFA) competes with P_i binding. Protons interact with the voltage-dependent transitions and final Na^+ binding. For electroneutral NaPi-IIc, the net mobile charge of the empty carrier is 0 and the 1st Na^+ interaction is absent. These transitions are replaced by an electroneutral transition (*2a-8a*). For NaPi-IIa/b, a Na^+-leak pathway (*2a-8a*), active in the absence of P_i, has also been characterized (2, 28, 29). This is undetectable in NaPi-IIc. The depicted mirror symmetries are speculative, and access to the intracellular milieu will be necessary to identify and characterize the transitions between the hypothesized internally oriented conformations. *B*: for PiT-1 proteins, experimental evidence suggests a mixed ordered/random binding scheme. As no pre-steady-state charge movement has so far been detected, we are unable to identify voltage-dependent transitions and tentatively assign the final reorientation of the fully loaded carrier (*4-5*, net charge +1) as the voltage-dependent transition.

Topology. The topology of PiT proteins has been partially determined (Fig. 5). Topology prediction algorithms usually report 9 or 11 transmembrane domains for PiT-1 and PiT-2, which would place the NH_2 and COOH termini on opposite sides of the membrane. However, tags inserted at the NH_2 and COOH termini are accessible from the external side, indicating that both termini are extracellular (24, 83, 86). A homological search (86) revealed the presence of a conserved domain in PiT proteins that is duplicated in most family members (light blue shading in Fig. 5). Reasoning that such duplicated sequences probably have similar but inverted topologies, Salaün et al. (86) proposed a secondary structure comprising extracellular NH_2 and COOH termini and 12 putative transmembrane domains (Fig. 5). They confirmed that *loop 2* is extracellular by showing that PiT-2 is *N*-glycosylated at Asp-81. The intracellular localization of the large *loop 7* was confirmed using an antibody raised against it (18). Similar topologies have been suggested for the malaria parasite transporter PfPiT (87) and for the related H^+/P_i transporter *Pht2;1* from the plant *Arabidopsis* (21). Interestingly, the plant protein is lacking the large intracellular loop present in animal PiTs. Furthermore, Bottger and Pedersen (9) showed that PiT2 retains its retroviral receptor function after deletion of *loop 7* as well as transmembrane domains 6–7 (pink shading in Fig. 5). They did not investigate the transport function of their truncated protein, and thus it is unknown whether the large loop is essential for substrate transport.

The ability of a retrovirus to infect cells via its receptor has been used extensively to investigate which amino acids are crucial for infection with different viruses and thus also serves as a tool for probing the secondary structure of PiTs. Most of the attention has been directed towards *loop 8* (Fig. 5). This shows large sequence variability between different species, and it appears to play a role in determining virus binding (22, 49, 77). Therefore, it is likely to be extracellular, although an opposing view has also been presented (24). The issue has been extensively discussed (8) in favor of the model proposed by Salaun et al. (86).

So far, only a few features of PiT topology have been experimentally confirmed, such as the location of the termini and *loops 2* and *7*. Salaun et al. (86) conducted in vitro translation experiments using PiT-2 constructs truncated at the COOH terminus. These data support the extracellular location of the four extracellular loops and the COOH terminus, whereas the other loops are intracellular. However, it is clear that further experiments are needed to establish a definitive membrane topology for PiT-1 and PiT-2, for example, by epitope tagging of putative loops or probing the accessibility of introduced cysteines to membrane-impermeant reagents, as done for the SLC34 protein.

Summary

In vertebrates, the two unrelated solute transport families SLC20 and SLC34 mediate Na^+/P_i cotransport through different molecular mechanisms. Their main functional properties are summarized in Table 1. It is remarkable that the two families have evolved a preference for one of the two P_i species that are most abundant at physiological pH, and thus both monovalent and divalent P_i species have their own dedicated carriers. Whether this functional difference between the two families has a strong impact on physiology is unclear. Note that transport of either P_i species across a membrane will affect pH, since it shifts the equilibrium of the reaction $H_2PO_4^-$ HPO_4^{2-} + H^+. An additional consequence is that the two families differ in their optimum pH range, overlapping around the pK_a of the above reaction (pH ~6.8). Thus SLC20, which prefers $H_2PO_4^-$, and SLC34, which prefers HPO_4^{2-}, transport most efficiently in the acidic and alkaline ranges, respectively (Fig. 6). This difference in preferred P_i species may explain why PFA inhibits P_i transport by SLC34, but not by SLC20.

The two families also differ in their substrate stoichiometry. NaPi-IIa and NaPi-IIb transport three Na^+ ions per transport cycle, concomitant with the translocation of one net positive charge, whereas NaPi-IIc only takes two Na^+ ions, resulting in electroneutral transport. Like NaPi-IIc also PiT transports two Na^+ ions per completed cycle, but because P_i is transported in its monovalent form, net positive charge is also translocated. These differences in stoichiometry and preferred P_i species result in a 100-fold difference in P_i concentration capacity from the lowest (NaPi-IIc, 100-fold) to the highest (NaPi-IIa and IIb, 10,000-fold; see Table 1). What are the physiological consequences of these differences in stoichiometry? Because NaPi-IIc transports one less Na^+ ion (resulting in electroneutral transport) than its electrogenic counterparts, the energetic cost of transporting P_i is smaller. Less Na^+ is loaded into the cell, and less energy is needed to maintain the cell's negative membrane potential.

With respect to substrate binding order (Fig. 7), SLC34 proteins appear to exhibit a strict Na^+-Na^+-P_i-Na^+ order (Fig. 7*A*), whereas the available evidence for SLC20 is less clear and random Na^+/P_i interactions cannot be excluded (81) (Fig. 7*B*). Moreover, the lack of detectable pre-steady-state currents in SLC20 prevents assigning voltage dependence to any particular step in the transport cycle, unlike for NaPi-IIa and IIb. This type of analysis assumes that pre-steady-state currents report on events that are associated with significant conformational changes related to the transport cycle; however, other scenarios are possible that would lead to the same macroscopic behavior. It is also conceivable that some of the pre-steady-state charge represents a conventional gating charge that precedes channel opening. In contrast to the canonical alternating access model, a channel-like "hopping" model, in which substrates move single file through a pore, successively occupying binding sites according to availability, was proposed, whereby the salient kinetic features of Na^+-coupled transport systems were predicted (92). Although several studies (40, 58) have argued against the validity of such a scheme in its purest form, the recent finding of a Cl^- channel that acts like a H^+/Cl^- antiport (1) indicates that channels and carriers may indeed share common mechanistic features.

ACKNOWLEDGMENTS

The authors acknowledge the valuable contributions made by past and present members of our laboratory.

GRANTS

Financial support for work cited from our laboratory was generously provided by the Swiss National Science Foundation and Gebert Rüf Foundation (www.grstiftung.ch).

REFERENCES

1. **Accardi A, Miller C.** Secondary active transport mediated by a prokaryotic homologue of ClC Cl^- channels. *Nature* 427: 803–807, 2004.
2. **Bacconi A, Ravera S, Virkki LV, Murer H, Forster IC.** Temperature-dependency of steady-state and presteady-state kinetics of a type IIb Na^+/P_i cotransporter. *J Membr Biol*. In press.
3. **Bacconi A, Virkki LV, Biber J, Murer H, Forster IC.** Renouncing electrogenicity is not free of charge: switching on electrogenicity in a Na^+-coupled phosphate cotransporter. *Proc Natl Acad Sci USA* 102: 12606–12611, 2005.
4. **Bai L, Collins JF, Ghishan FK.** Cloning and characterization of a type III Na-dependent phosphate cotransporter from mouse intestine. *Am J Physiol Cell Physiol* 279: C1135–C1143, 2000.
5. **Beck L, Karaplis AC, Amizuka N, Hewson AS, Ozawa H, Tenenhouse HS.** Targeted inactivation of Npt2 in mice leads to severe renal phosphate wasting, hypercalciuria, and skeletal abnormalities. *Proc Natl Acad Sci USA* 95: 5372–5377, 1998.
6. **Bellocchio EE, Reimer RJ, Fremeau RT Jr, Edwards RH.** Uptake of glutamate into synaptic vesicles by an inorganic phosphate transporter. *Science* 289: 957–960, 2000.
7. **Bergwitz C, Roslin NM, Tieder M, Loredo-Osti JC, Bastepe M, Abu-Zahra H, Frappier D, Burkett K, Carpenter TO, Anderson D, Garabedian M, Sermet I, Fujiwara TM, Morgan K, Tenenhouse HS, Juppner H.** SLC34A3 mutations in patients with hereditary hypophosphatemic rickets with hypercalciuria predict a key role for the sodium-phosphate cotransporter NaPi-IIc in maintaining phosphate homeostasis. *Am J Hum Genet* 78: 179–192, 2006.
8. **Bottger P, Hede SE, Grunnet M, Hoyer B, Klaerke DA, Pedersen L.** Characterization of transport mechanisms and determinants critical for Na^+-dependent P_i symport of the PiT-family paralogs, human PiT1 and PiT2. *Am J Physiol Cell Physiol* 291: C1377–C1387, 2006.
9. **Bottger P, Pedersen L.** The central half of Pit2 is not required for its function as a retroviral receptor. *J Virol* 78: 9564–9567, 2004.
10. **Bottger P, Pedersen L.** Evolutionary and experimental analyses of inorganic phosphate transporter PiT family reveals two related signature sequences harboring highly conserved aspartic acids critical for sodium-dependent phosphate transport function of human PiT2. *FEBS J* 272: 3060–3074, 2005.
11. **Bottger P, Pedersen L.** Two highly conserved glutamate residues critical for type III sodium-dependent phosphate transport revealed by uncoupling transport function from retroviral receptor function. *J Biol Chem* 277: 42741–42747, 2002.
12. **Burckhardt G, Stern H, Murer H.** The influence of pH on phosphate transport into rat renal brush border membrane vesicles. *Pflügers Arch* 390: 191–197, 1981.
13. **Busch A, Waldegger S, Herzer T, Biber J, Markovich D, Hayes G, Murer H, Lang F.** Electrophysiological analysis of Na^+/P_i cotransport mediated by a transporter cloned from rat kidney and expressed in *Xenopus* oocytes. *Proc Natl Acad Sci USA* 91: 8205–8208, 1994.
14. **Busch AE, Schuster A, Waldegger S, Wagner CA, Zempel G, Broer S, Biber J, Murer H, Lang F.** Expression of a renal type I sodium/phosphate transporter (NaPi-1) induces a conductance in *Xenopus* oocytes permeable for organic and inorganic anions. *Proc Natl Acad Sci USA* 93: 5347–5351, 1996.
15. **Busch AE, Wagner CA, Schuster A, Waldegger S, Biber J, Murer H, Lang F.** Properties of electrogenic P_i transport by a human renal brush border Na^+/P_i transporter. *J Am Soc Nephrol* 6: 1547–1551, 1995.
16. **Caverzasio J, Bonjour JP.** Characteristics and regulation of Pi transport in osteogenic cells for bone metabolism. *Kidney Int* 49: 975–980, 1996.
17. **Cecil DL, Rose DM, Terkeltaub R, Liu-Bryan R.** Role of interleukin-8 in PiT-1 expression and CXCR1-mediated inorganic phosphate uptake in chondrocytes. *Arthritis Rheum* 52: 144–154, 2005.
18. **Chien ML, Foster JL, Douglas JL, Garcia JV.** The amphotropic murine leukemia virus receptor gene encodes a 71-kilodalton protein that is induced by phosphate depletion. *J Virol* 71: 4564–4570, 1997.
19. **Collins JF, Bai L, Ghishan FK.** The SLC20 family of proteins: dual functions as sodium-phosphate cotransporters and viral receptors. *Pflügers Arch* 447: 647–652, 2004.
20. **Corut A, Senyigit A, Ugur SA, Altin S, Ozcelik U, Calisir H, Yildirim Z, Gocmen A, Tolun A.** Mutations in SLC34A2 cause pulmonary alveolar microlithiasis and are possibly associated with testicular microlithiasis. *Am J Hum Genet* 79: 650–656, 2006.
21. **Daram P, Brunner S, Rausch C, Steiner C, Amrhein N, Bucher M.** Pht2;1 encodes a low-affinity phosphate transporter from *Arabidopsis*. *Plant Cell* 11: 2153–2166, 1999.
22. **Dreyer K, Pedersen FS, Pedersen L.** A 13-amino-acid Pit1-specific loop 4 sequence confers feline leukemia virus subgroup B receptor function upon Pit2. *J Virol* 74: 2926–2929, 2000.
23. **Eskandari S, Loo DD, Dai G, Levy O, Wright EM, Carrasco N.** Thyroid Na^+/I symporter. Mechanism, stoichiometry, specificity. *J Biol Chem* 272: 27230–27238, 1997.
24. **Farrell KB, Russ JL, Murthy RK, Eiden MV.** Reassessing the role of region A in Pit1-mediated viral entry. *J Virol* 76: 7683–7693, 2002.
25. **Fernandes I, Beliveau R, Friedlander G, Silve C.** $NaPO_4$ cotransport type III (PiT1) expression in human embryonic kidney cells and regulation by PTH. *Am J Physiol Renal Physiol* 277: F543–F551, 1999.
26. **Fleisch H.** Bisphosphonates: mechanisms of action. *Endocr Rev* 19: 80–100, 1998.
27. **Fleisch HA, Russell RG, Bisaz S, Muhlbauer RC, Williams DA.** The inhibitory effect of phosphonates on the formation of calcium phosphate crystals in vitro and on aortic and kidney calcification in vivo. *Eur J Clin Invest* 1: 12–18, 1970.
28. **Forster I, Hernando N, Biber J, Murer H.** The voltage dependence of a cloned mammalian renal type II Na^+/P_i cotransporter (NaPi-2). *J Gen Physiol* 112: 1–18, 1998.
29. **Forster IC, Biber J, Murer H.** Proton-sensitive transitions of renal type II Na^+-coupled phosphate cotransporter kinetics. *Biophys J* 79: 215–230, 2000.
30. **Forster IC, Hernando N, Biber J, Murer H.** Proximal tubular handling of phosphate: a molecular perspective. *Kidney Int* 70: 1548–1559, 2006.
31. **Forster IC, Kohler K, Biber J, Murer H.** Forging the link between structure and function of electrogenic cotransporters: the renal type IIa Na^+/P_i cotransporter as a case study. *Prog Biophys Mol Biol* 80: 69–108, 2002.
32. **Forster IC, Loo DD, Eskandari S.** Stoichiometry and Na^+ binding cooperativity of rat and flounder renal type II Na^+-P_i cotransporters. *Am J Physiol Renal Physiol* 276: F644–F649, 1999.
33. **Forster IC, Wagner CA, Busch AE, Lang F, Biber J, Hernando N, Murer H, Werner A.** Electrophysiological characterization of the flounder type II Na^+/P_i cotransporter (NaPi-5) expressed in *Xenopus laevis* oocytes. *J Membr Biol* 160: 9–25, 1997.
34. **Frappart L, Boudeulle M, Boumendil J, Lin HC, Martinon I, Palayer C, Mallet-Guy Y, Raudrant D, Bremond A, Rochet Y.** Structure and composition of microcalcifications in benign and malignant lesions of the breast: study by light microscopy, transmission and scanning electron microscopy, microprobe analysis, and X-ray diffraction. *Hum Pathol* 15: 880–889, 1984.
35. **Frei P, Gao B, Hagenbuch B, Mate A, Biber J, Murer H, Meier PJ, Stieger B.** Identification and localization of sodium-phosphate cotransporters in hepatocytes and cholangiocytes of rat liver. *Am J Physiol Gastrointest Liver Physiol* 288: G771–G778, 2005.
36. **Guicheux J, Palmer G, Shukunami C, Hiraki Y, Bonjour JP, Caverzasio J.** A novel in vitro culture system for analysis of functional role of phosphate transport in endochondral ossification. *Bone* 27: 69–74, 2000.
37. **Gupta A, Tenenhouse HS, Hoag HM, Wang D, Khadeer MA, Namba N, Feng X, Hruska KA.** Identification of the type II Na^+-P_i cotransporter (Npt2) in the osteoclast and the skeletal phenotype of Npt2−/− mice. *Bone* 29: 467–476, 2001.
38. **Harris RM, Webb DC, Howitt SM, Cox GB.** Characterization of PitA and PitB from *Escherichia coli*. *J Bacteriol* 183: 5008–5014, 2001.
39. **Hartmann CM, Wagner CA, Busch AE, Markovich D, Biber J, Lang F, Murer H.** Transport characteristics of a murine renal Na/Pi-cotransporter. *Pflügers Arch* 430: 830–836, 1995.
40. **Hazama A, Loo DD, Wright EM.** Presteady-state currents of the rabbit Na^+/glucose cotransporter (SGLT1). *J Membr Biol* 155: 175–186, 1997.
41. **Hernando N, Gisler SM, Pribanic S, Deliot N, Capuano P, Wagner CA, Moe OW, Biber J, Murer H.** NaPi-IIa and interacting partners. *J Physiol* 567: 21–26, 2005.
42. **Hilfiker H, Hattenhauer O, Traebert M, Forster I, Murer H, Biber J.** Characterization of a murine type II sodium-phosphate cotransporter expressed in mammalian small intestine. *Proc Natl Acad Sci USA* 95: 14564–14569, 1998.
43. **Hirayama BA, Loo DD, Wright EM.** Cation effects on protein conformation and transport in the Na^+/glucose cotransporter. *J Biol Chem* 272: 2110–2115, 1997.

44. **Hisano S, Haga H, Li Z, Tatsumi S, Miyamoto KI, Takeda E, Fukui Y.** Immunohistochemical and RT-PCR detection of Na^+-dependent inorganic phosphate cotransporter (NaPi-2) in rat brain. *Brain Res* 772: 149–155, 1997.
45. **Homann V, Rosin-Steiner S, Stratmann T, Arnold WH, Gaengler P, Kinne RK.** Sodium-phosphate cotransporter in human salivary glands: molecular evidence for the involvement of NPT2b in acinar phosphate secretion and ductal phosphate reabsorption. *Arch Oral Biol* 50: 759–768, 2005.
46. **Huqun Izumi S, Miyazawa H, Ishii K, Uchiyama B, Ishida T, Tanaka S, Tazawa R, Fukuyama S, Tanaka T, Nagai Y, Yokote A, Takahashi H, Fukushima T, Kobayashi K, Chiba H, Nagata M, Sakamoto S, Nakata K, Hagiwara K.** Mutations in the SLC34A2 gene are associated with the pulmonary alveolar microlithiasis. *Am J Respir Crit Care Med* 175: 263–268, 2006.
47. **Ichikawa S, Sorenson AH, Imel EA, Friedman NE, Gertner JM, Econs MJ.** Intronic deletions in the SLC34A3 gene cause hereditary hypophosphatemic rickets with hypercalciuria. *J Clin Endocrinol Metab* 91: 4022–4027, 2006.
48. **Johann SV, Gibbons JJ, O'Hara B.** GLVR1, a receptor for gibbon ape leukemia virus, is homologous to a phosphate permease of *Neurospora crassa* and is expressed at high levels in the brain and thymus. *J Virol* 66: 1635–1640, 1992.
49. **Johann SV, van Zeijl M, Cekleniak J, O'Hara B.** Definition of a domain of GLVR1 which is necessary for infection by gibbon ape leukemia virus and which is highly polymorphic between species. *J Virol* 67: 6733–6736, 1993.
50. **Jono S, McKee MD, Murry CE, Shioi A, Nishizawa Y, Mori K, Morii H, Giachelli CM.** Phosphate regulation of vascular smooth muscle cell calcification. *Circ Res* 87: E10–E17, 2000.
51. **Kavanaugh MP, Kabat D.** Identification and characterization of a widely expressed phosphate transporter/retrovirus receptor family. *Kidney Int* 49: 959–963, 1996.
52. **Kavanaugh MP, Miller DG, Zhang W, Law W, Kozak SL, Kabat D, Miller AD.** Cell-surface receptors for gibbon ape leukemia virus and amphotropic murine retrovirus are inducible sodium-dependent phosphate symporters. *Proc Natl Acad Sci USA* 91: 7071–7075, 1994.
53. **Khadeer MA, Tang Z, Tenenhouse HS, Eiden MV, Murer H, Hernando N, Weinman EJ, Chellaiah MA, Gupta A.** Na^+-dependent phosphate transporters in the murine osteoclast: cellular distribution and protein interactions. *Am J Physiol Cell Physiol* 284: C1633–C1644, 2003.
54. **Kohler K, Forster IC, Lambert G, Biber J, Murer H.** The functional unit of the renal type IIa Na^+/Pi cotransporter is a monomer. *J Biol Chem* 275: 26113–26120, 2000.
55. **Lapointe JY, Tessier J, Paquette Y, Wallendorff B, Coady MJ, Pichette V, Bonnardeaux A.** NPT2a gene variation in calcium nephrolithiasis with renal phosphate leak. *Kidney Int* 69: 2261–2267, 2006.
56. **Li X, Yang HY, Giachelli CM.** Role of the sodium-dependent phosphate cotransporter, Pit-1, in vascular smooth muscle cell calcification. *Circ Res* 98: 905–912, 2006.
57. **Lorenz-Depiereux B, Benet-Pages A, Eckstein G, Tenenbaum-Rakover Y, Wagenstaller J, Tiosano D, Gershoni-Baruch R, Albers N, Lichtner P, Schnabel D, Hochberg Z, Strom TM.** Hereditary hypophosphatemic rickets with hypercalciuria is caused by mutations in the sodium-phosphate cotransporter gene SLC34A3. *Am J Hum Genet* 78: 193–201, 2006.
58. **Lu CC, Hilgemann DW.** GAT1 (GABA:Na^+:Cl^-) cotransport function. Steady state studies in giant *Xenopus* oocyte membrane patches. *J Gen Physiol* 114: 429–444, 1999.
59. **Lundquist P, Biber J, Murer H.** Type II Na^+-P_i cotransporters in osteoblast mineral formation: regulation by inorganic phosphate. *Cell Physiol Biochem* 19: 43–56, 2007.
60. **Madjdpour C, Bacic D, Kaissling B, Murer H, Biber J.** Segment-specific expression of sodium-phosphate cotransporters NaPi-IIa and -IIc and interacting proteins in mouse renal proximal tubules. *Pflügers Arch* 448: 402–410, 2004.
61. **Magagnin S, Werner A, Markovich D, Sorribas V, Stange G, Biber J, Murer H.** Expression cloning of human and rat renal cortex Na/P_i cotransport. *Proc Natl Acad Sci USA* 90: 5979–5983, 1993.
62. **Mansfield K, Teixeira CC, Adams CS, Shapiro IM.** Phosphate ions mediate chondrocyte apoptosis through a plasma membrane transporter mechanism. *Bone* 28: 1–8, 2001.
63. **Mansilla MC, de Mendoza D.** The *Bacillus subtilis* cysP gene encodes a novel sulphate permease related to the inorganic phosphate transporter (Pit) family. *Microbiology* 146: 815–821, 2000.
64. **Martinez P, Persson BL.** Identification, cloning and characterization of a derepressible Na^+-coupled phosphate transporter in Saccharomyces cerevisiae. *Mol Gen Genet* 258: 628–638, 1998.
65. **Miller DG, Edwards RH, Miller AD.** Cloning of the cellular receptor for amphotropic murine retroviruses reveals homology to that for gibbon ape leukemia virus. *Proc Natl Acad Sci USA* 91: 78–82, 1994.
66. **Miyamoto K, Segawa H, Ito M, Kuwahata M.** Physiological regulation of renal sodium-dependent phosphate cotransporters. *Jpn J Physiol* 54: 93–102, 2004.
67. **Miyoshi K, Shillingford JM, Smith GH, Grimm SL, Wagner KU, Oka T, Rosen JM, Robinson GW, Hennighausen L.** Signal transducer and activator of transcription (Stat) 5 controls the proliferation and differentiation of mammary alveolar epithelium. *J Cell Biol* 155: 531–542, 2001.
68. **Mizobuchi M, Ogata H, Hatamura I, Koiwa F, Saji F, Shiizaki K, Negi S, Kinugasa E, Ooshima A, Koshikawa S, Akizawa T.** Up-regulation of Cbfa1 and Pit-1 in calcified artery of uraemic rats with severe hyperphosphataemia and secondary hyperparathyroidism. *Nephrol Dial Transplant* 21: 911–916, 2006.
69. **Mulroney SE, Woda CB, Halaihel N, Louie B, McDonnell K, Schulkin J, Haramati A, Levi M.** Central control of renal sodium-phosphate (NaPi-2) transporters. *Am J Physiol Renal Physiol* 286: F647–F652, 2004.
70. **Murer H, Hernando N, Forster I, Biber J.** Proximal tubular phosphate reabsorption: molecular mechanisms. *Physiol Rev* 80: 1373–1409, 2000.
71. **Ohkido I, Segawa H, Yanagida R, Nakamura M, Miyamoto K.** Cloning, gene structure and dietary regulation of the type-IIc Na/Pi cotransporter in the mouse kidney. *Pflügers Arch* 446: 106–115, 2003.
72. **Olah Z, Lehel C, Anderson WB, Eiden MV, Wilson CA.** The cellular receptor for gibbon ape leukemia virus is a novel high affinity sodium-dependent phosphate transporter. *J Biol Chem* 269: 25426–25431, 1994.
73. **Pajor AM, Hirayama BA, Loo DD.** Sodium and lithium interactions with the Na^+/dicarboxylate cotransporter. *J Biol Chem* 273: 18923–18929, 1998.
74. **Palmer G, Guicheux J, Bonjour JP, Caverzasio J.** Transforming growth factor-beta stimulates inorganic phosphate transport and expression of the type III phosphate transporter Glvr-1 in chondrogenic ATDC5 cells. *Endocrinology* 141: 2236–2243, 2000.
75. **Palmer G, Zhao J, Bonjour J, Hofstetter W, Caverzasio J.** In vivo expression of transcripts encoding the Glvr-1 phosphate transporter/retrovirus receptor during bone development. *Bone* 24: 1–7, 1999.
76. **Parent L, Supplisson S, Loo DD, Wright EM.** Electrogenic properties of the cloned Na^+/glucose cotransporter: II. A transport model under nonrapid equilibrium conditions. *J Membr Biol* 125: 63–79, 1992.
77. **Pedersen L, van Zeijl M, Johann SV, O'Hara B.** Fungal phosphate transporter serves as a receptor backbone for gibbon ape leukemia virus. *J Virol* 71: 7619–7622, 1997.
78. **Prie D, Huart V, Bakouh N, Planelles G, Dellis O, Gerard B, Hulin P, Benque-Blanchet F, Silve C, Grandchamp B, Friedlander G.** Nephrolithiasis and osteoporosis associated with hypophosphatemia caused by mutations in the type 2a sodium-phosphate cotransporter. *N Engl J Med* 347: 983–991, 2002.
79. **Radanovic T, Gisler SM, Biber J, Murer H.** Topology of the type II Na^+/P_i-cotransporter. *J Membr Biol* 212: 41–49, 2006.
80. **Radanovic T, Wagner CA, Murer H, Biber J.** Regulation of intestinal phosphate transport. I. Segmental expression and adaptation to low-P_i diet of the type IIb Na^+-P_i cotransporter in mouse small intestine. *Am J Physiol Gastrointest Liver Physiol* 288: G496–G500, 2005.
81. **Ravera S, Virkki LV, Murer H, Forster IC.** Deciphering PiT transport kinetics and substrate specificity using electrophysiology and flux measurements. *Am J Physiol Cell Physiol*. First published May 9, 2007; doi:10.1152/ajpcell.00064. 2007.
82. **Reimer RJ, Edwards RH.** Organic anion transport is the primary function of the SLC17/type I phosphate transporter family. *Pflügers Arch* 447: 629–635, 2004.
83. **Rodrigues P, Heard JM.** Modulation of phosphate uptake and amphotropic murine leukemia virus entry by posttranslational modifications of PIT-2. *J Virol* 73: 3789–3799, 1999.
84. **Salaun C, Gyan E, Rodrigues P, Heard JM.** Pit2 assemblies at the cell surface are modulated by extracellular inorganic phosphate concentration. *J Virol* 76: 4304–4311, 2002.

85. **Salaun C, Marechal V, Heard JM.** Transport-deficient Pit2 phosphate transporters still modify cell surface oligomers structure in response to inorganic phosphate. *J Mol Biol* 340: 39–47, 2004.
86. **Salaun C, Rodrigues P, Heard JM.** Transmembrane topology of PiT-2, a phosphate transporter-retrovirus receptor. *J Virol* 75: 5584–5592, 2001.
87. **Saliba KJ, Martin RE, Broer A, Henry RI, McCarthy CS, Downie MJ, Allen RJ, Mullin KA, McFadden GI, Broer S, Kirk K.** Sodium-dependent uptake of inorganic phosphate by the intracellular malaria parasite. *Nature* 443: 582–585, 2006.
88. **Samarzija I, Molnar V, Fromter E.** pH-dependence of phosphate absorption in rat renal proximal tubule. *Proc Eur Dial Transplant Assoc* 19: 779–783, 1983.
89. **Segawa H, Kaneko I, Takahashi A, Kuwahata M, Ito M, Ohkido I, Tatsumi S, Miyamoto K.** Growth-related renal type II Na/Pi cotransporter. *J Biol Chem* 277: 19665–19672, 2002.
90. **Shillingford JM, Calvert DT, Beechey RB, Shennan DB.** Phosphate transport via Na^+ -P_i cotransport and anion exchange in lactating rat mammary tissue. *Exp Physiol* 81: 273–284, 1996.
91. **Stauber A,Radanovic T, Stange G, Murer H, Wagner CA, Biber J.** Regulation of intestinal phosphate transport. II. Metabolic acidosis stimulates Na^+-dependent phosphate absorption and expression of the Na^+-P_i cotransporter NaPi-IIb in small intestine. *Am J Physiol Gastrointest Liver Physiol* 288: G501–G506, 2005.
92. **Su A, Mager S, Mayo SL, Lester HA.** A multi-substrate single-file model for ion-coupled transporters. *Biophys J* 70: 762–777, 1996.
93. **Suzuki A, Ghayor C, Guicheux J, Magne D, Quillard S, Kakita A, Ono Y, Miura Y, Oiso Y, Itoh M, Caverzasio J.** Enhanced expression of the inorganic phosphate transporter Pit-1 is involved in BMP-2-induced matrix mineralization in osteoblast-like cells. *J Bone Miner Res* 21: 674–683, 2006.
94. **Suzuki A, Palmer G, Bonjour JP, Caverzasio J.** Stimulation of sodium-dependent inorganic phosphate transport by activation of Gi/o-protein-coupled receptors by epinephrine in MC3T3-E1 osteoblast-like cells. *Bone* 28: 589–594, 2001.
95. **Suzuki A, Palmer G, Bonjour JP, Caverzasio J.** Stimulation of sodium-dependent phosphate transport and signaling mechanisms induced by basic fibroblast growth factor in MC3T3–E1 osteoblast-like cells. *J Bone Miner Res* 15: 95–102, 2000.
96. **Szczepanska-Konkel M, Yusufi AN, VanScoy M, Webster SK, Dousa TP.** Phosphonocarboxylic acids as specific inhibitors of Na^+-dependent transport of phosphate across renal brush border membrane. *J Biol Chem* 261: 6375–6383, 1986.
97. **Tatsumi S, Segawa H, Morita K, Haga H, Kouda T, Yamamoto H, Inoue Y, Nii T, Katai K, Taketani Y, Miyamoto KI, Takeda E.** Molecular cloning and hormonal regulation of PiT-1, a sodium-dependent phosphate cotransporter from rat parathyroid glands. *Endocrinology* 139: 1692–1699, 1998.
98. **Tenenhouse HS.** Regulation of phosphorus homeostasis by the type IIa Na/phosphate cotransporter. *Annu Rev Nutr* 25: 197–214, 2005.
99. **Tenenhouse HS, Gauthier C, Martel J, Gesek FA, Coutermarsh BA, Friedman PA.** Na^+-phosphate cotransport in mouse distal convoluted tubule cells: evidence for Glvr-1 and Ram-1 gene expression. *J Bone Miner Res* 13: 590–597, 1998.
100. **Tenenhouse HS, Murer H.** Disorders of renal tubular phosphate transport. *J Am Soc Nephrol* 14: 240–248, 2003.
101. **Traebert M, Hattenhauer O, Murer H, Kaissling B, Biber J.** Expression of type II Na-P_i cotransporter in alveolar type II cells. *Am J Physiol Lung Cell Mol Physiol* 277: L868–L873, 1999.
102. **Uckert W, Willimsky G, Pedersen FS, Blankenstein T, Pedersen L.** RNA levels of human retrovirus receptors Pit1 and Pit2 do not correlate with infectibility by three retroviral vector pseudotypes. *Hum Gene Ther* 9: 2619–2627, 1998.
103. **van Veen HW.** Phosphate transport in prokaryotes: molecules, mediators and mechanisms. *Antonie Van Leeuwenhoek* 72: 299–315, 1997.
104. **van Zeijl M, Johann SV, Closs E, Cunningham J, Eddy R, Shows TB, O'Hara B.** A human amphotropic retrovirus receptor is a second member of the gibbon ape leukemia virus receptor family. *Proc Natl Acad Sci USA* 91: 1168–1172, 1994.
105. **Vayro S, Kemp R, Beechey RB, Shirazi-Beechey S.** Preparation and characterization of basolateral plasma-membrane vesicles from sheep parotid glands. Mechanisms of phosphate and D-glucose transport. *Biochem J* 279: 843–848, 1991.
106. **Versaw WK, Metzenberg RL.** Repressible cation-phosphate symporters in *Neurospora crassa*. *Proc Natl Acad Sci USA* 92: 3884–3887, 1995.
107. **Villa-Bellosta R, Bogaert YE, Levi M, Sorribas V.** Characterization of phosphate transport in rat vascular smooth muscle cells: implications for vascular calcification. *Arterioscler Thromb Vasc Biol* 27: 1030–1036, 2007.
108. **Virkki LV, Choi I, Davis BA, Boron WF.** Cloning of a Na^+-driven Cl/HCO_3 exchanger from squid giant fiber lobe. *Am J Physiol Cell Physiol* 285: C771–C780, 2003.
109. **Virkki LV, Forster IC, Bacconi A, Biber J, Murer H.** Functionally important residues in the predicted 3rd transmembrane domain of the type IIa sodium-phosphate co-transporter (NaPi-IIa). *J Membr Biol* 206: 227–238, 2005.
110. **Virkki LV, Forster IC, Biber J, Murer H.** Substrate interactions in the human type IIa sodium-phosphate cotransporter (NaPi-IIa). *Am J Physiol Renal Physiol* 288: F969–F981, 2005.
111. **Virkki LV, Forster IC, Hernando N, Biber J, Murer H.** Functional characterization of two naturally occurring mutations in the human sodium-phosphate cotransporter type IIa. *J Bone Miner Res* 18: 2135–2141, 2003.
112. **Virkki LV, Murer H, Forster IC.** Mapping conformational changes of the type IIb Na^+/P_i cotransporter by voltage clamp fluorometry. *J Biol Chem* 281: 28837–28849, 2006.
113. **Virkki LV, Murer H, Forster IC.** Voltage clamp fluorometric measurements on a type II Na^+-coupled P_i cotransporter: shedding light on substrate binding order. *J Gen Physiol* 127: 539–555, 2006.
114. **Wang D, Canaff L, Davidson D, Corluka A, Liu H, Hendy GN, Henderson JE.** Alterations in the sensing and transport of phosphate and calcium by differentiating chondrocytes. *J Biol Chem* 276: 33995–34005, 2001.
115. **Wang G, Williams G, Xia H, Hickey M, Shao J, Davidson BL, McCray PB.** Apical barriers to airway epithelial cell gene transfer with amphotropic retroviral vectors. *Gene Ther* 9: 922–931, 2002.
116. **Werner A, Kinne RK.** Evolution of the Na-P_i cotransport systems. *Am J Physiol Regul Integr Comp Physiol* 280: R301–R312, 2001.
117. **Werner A, Moore ML, Mantei N, Biber J, Semenza G, Murer H.** Cloning and expression of cDNA for a Na/Pi cotransport system of kidney cortex. *Proc Natl Acad Sci USA* 88: 9608–9612, 1991.
118. **Williams G, Sallis JD.** Structure-activity relationship of inhibitors of hydroxyapatite formation. *Biochem J* 184: 181–184, 1979.
119. **Xu H, Inouye M, Missey T, Collins JF, Ghishan FK.** Functional characterization of the human intestinal NaPi-IIb cotransporter in hamster fibroblasts and *Xenopus* oocytes. *Biochim Biophys Acta* 1567: 97–105, 2002.
120. **Xu Y, Yeung CH, Setiawan I, Avram C, Biber J, Wagenfeld A, Lang F, Cooper TG.** Sodium-inorganic phosphate cotransporter NaPi-IIb in the epididymis and its potential role in male fertility studied in a transgenic mouse model. *Biol Reprod* 69: 1135–1141, 2003.
121. **Yoshiko Y, Candeliere GA, Maeda N, Aubin JE.** Osteoblast autonomous Pi regulation via Pit1 plays a role in bone mineralization. *Mol Cell Biol* 27: 4465–4474, 2007.
122. **Zhen X, Bonjour JP, Caverzasio J.** Platelet-derived growth factor stimulates sodium-dependent Pi transport in osteoblastic cells via phospholipase Cgamma and phosphatidylinositol 3′-kinase. *J Bone Miner Res* 12: 36–44, 1997.
123. **Zoidis E, Ghirlanda-Keller C, Gosteli-Peter M, Zapf J, Schmid C.** Regulation of phosphate (P_i) transport and NaPi-III transporter (Pit-1) mRNA in rat osteoblasts. *J Endocrinol* 181: 531–540, 2004.